*Environ. Sci. Technol.* **1999**, *33,* 1293−1299

# Applications of Microelectrode Techniques To Measure pH and Oxidation−Reduction Potential in Rhizosphere Soil

TIAN C. ZHANG* AND HUI PANG

*Department of Civil Engineering, University of Nebraska−Lincoln at Omaha Campus, Omaha, Nebraska 68182-0178*

Microelectrodes are powerful analytical tools that can be used to measure microscale environments in rhizosphere soil. In this study, custom-made microelectrodes were used to measure pH and oxidation−reduction potential (ORP or redox potential) distributions in vegetated and unvegetated munitions-contaminated soils. While pH was essentially uniform in unvegetated soil, in the vegetated soil the pH was lower near the root tips than at other locations around the root. The pH varied little in the radial (horizontal) direction but was highest (pH = 6.20) near the surface (0.5 cm depth) and lowest (pH = 4.99) at 6 cm below the soil surface. There was a strong correlation between the redox potential and pH. Therefore, redox potentials were normalized to pH 7 based on an experimentally obtained ORP-pH curve. In the vegetated soil, the redox potentials increased as the center of the plant was approached. The highest ($ORP_7$ = 256 mV) and lowest ($ORP_7$ = 191 mV) redox potentials were measured at 0.5 and 3 cm below the surface of the soil, respectively. In the unvegetated soil, redox potential decreased with depth, which can be attributed to reduced transport of oxygen from the air to soil.

## Introduction

It is well-known that rhizosphere environment differs from the bulk soil. The plant-soil rhizosphere is characterized by radial and longitudinal gradients along individual roots (*1*). The rhizosphere environment and the extent to which roots and associated microfauna modify this environment are critical to nutrient uptake, transformation of xenobiotics, and adaptation of plants to adverse soil chemical perturbations. Characterizing rhizosphere conditions has been limited to macroscopic observations, due to the difficulty in measuring rhizosphere environments on a microscopic scale in situ.

The microelectrode technique is a powerful tool that can be used to characterize rhizosphere microenvironments. This technique has been traditionally used in neurobiology to measure intracellular and extracellular conditions, such as the electrical potential across the membrane of the cell and the transmembrane signals evoked during normal cellular activity, etc. (*2, 3*). Recently, microelectrode techniques have become one of the most powerful analytical methods to characterize chemical and metabolic activity gradients in biofilms (*4*−*12*) and for investigating competition between bacteria for space and substrate within biofilms (*13*−*15*). The microelectrode technique has also been used to study transport phenomena in biofilms (*16, 17*), biocatalyst particles (*18*), an immobilized $O_2$ reducing enzyme (*19*), plant roots (*20*), and flow regimes (*21, 22*). More importantly, researchers at the Center for Biofilm Engineering at the Montana State University have used microelectrode techniques, together with other techniques, to study biofilm structures (*23, 24*), local mass transfer coefficient in biofilms (*25*−*27*), biocide action against biofilms (*28, 29*), and other very important areas related to biofilms (*30, 31*).

Although some pioneering work has been conducted on oxidation−reduction potentials (ORPs or redox potentials) in biofilm systems using microelectrode techniques (*32*−*34*), up to now, very few studies have been conducted to investigate microscale environments in vegetated or unvegetated soils. Sextone et al. (*35*) used $O_2$ microelectrodes with a sensing tip size of 1−3 $\mu$m to measure oxygen profiles and denitrification rates in soil aggregates. Flessa and Fischer (*36*) used redox potential microelectrodes with a Pt wire (0.5 mm in diameter) to measure redox in microsites of the rhizosphere of flooded rice and found redox potential markedly increased close to the root tips. Conkling and Blanchar (*37*) and Yang et al. (*38, 39*) used glass microelectrodes to measure microscale pH spatial distributions in soil cores. They measured soil heterogeneity and reported that the spatial dependence of pH in microenvironments varied with sampling site and scale.

Despite the aforementioned studies, information is still lacking on the application of microelectrode techniques for measuring microscale environments in rhizosphere. In this study, microelectrode techniques were used to measure pH and redox potential in the rhizosphere. This paper presents detailed information on the experimental system design, improvement of the pH microelectrode for measuring soil samples, and the application of microelectrodes to measure pH and redox potential distributions in soil contaminated with TNT (2,4,6-trinitrotoluene) and RDX (hexahydro-1,3,5-trinitro-1,3,5-triazine).

## Materials and Methods

**Soil Samples.** Vegetated and unvegetated munitions-contaminated soils were obtained from the former Nebraska Ordnance plant (Mead, NE). This was a military loading and packing facility that produced bombs, boosters, and shells during World War II and the Korean War. TNT and RDX concentrations in the soil were determined using an HPLC method (*40*). Unvegetated soil was obtained from a barren area, probably due to high concentrations of TNT (4564 mg TNT/kg) and RDX (4488 mg RDX/kg). Plant growth in adjacent soil indicated a capacity to tolerate lower concentration of TNT (20 mg/kg) and RDX (285 mg/kg). Daisy fleabane (*Erigeron strigosus*) plants and surrounding soil were collected as "vegetated soil" samples. In the laboratory, both vegetated and unvegetated soils were watered for 10 days before initiating the experiment.

**Experimental Design.** To characterize pH and redox potentials in the soil near the plant roots, a 10 × 10 × 10 cm core was cut around the center of the plant (Figure 1). Along the vertical central line of each side, four points were measured at 0.5 (H1), 3 (H2), 6 (H3), and 9 cm (H4) below the soil surface. Following the initial 16 sampling points (four points on each side for pH and redox potential), the samplings were repeated by reducing the rectangular soil core to 7.5 × 7.5 × 10 cm, and subsequently to 5 × 5 × 10 cm, and finally to 2.5 × 2.5 × 10 cm, with no change in core height. At each

* Corresponding author phone: (402)554-3784; fax: (402)554-3288; e-mail: tzhang@unomaha.edu.

10.1021/es981070x CCC: $18.00 
Published on Web 02/27/1999

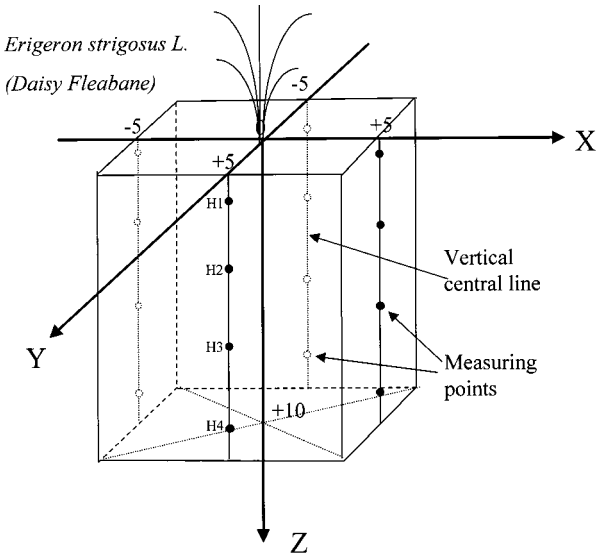


**FIGURE 1. Schematic diagram of sampling scheme.**

sampling point, the redox potential was measured first, followed by pH. The microelectrode penetrated 3−4 mm into the soil core. Measurements obtained from the outer three cores (10, 7.5, and 5 cm) were interpreted as pH and redox potential distributions in soil root areas (soil around the plant) but not within the rhizosphere. The core nearest the plant (2.5 cm) had the highest root density and for discussion purposes; measurements taken at these sampling points (ca. 2−3 mm from roots) are assumed to represent the rhizosphere.

For unvegetated soil, three columns with a diameter of 5 cm and a height of 10 cm were collected at three randomly chosen sites devoid of vegetation. For each column, pH and redox potential were measured at 0.5 (H1), 3 (H2), 6 (H3), and 9 cm (H4) below the soil surface.

**Suitable Microelectrode Tip Size.** Tests were conducted to determine a suitable microelectrode tip size (outside diameter, o.d.). Microelectrode tips (1−5 $\mu$m) described in the literature are mainly for cell and biofilm samples, which are soft and have a high water content. The harder and drier soil may break the microelectrode tip. Accordingly, artificial soils, consisting of sand, clay, and water, were used to investigate the effects of soil compositions and moisture content on microelectrode tips varying in size. The pulled glass probe (o.d. usually < 1 $\mu$m) was controlled by a 3-D manual manipulator (World Precision Instrument, Sarasota, FL) to penetrate the soils (usually 5−10 mm deep into the soil). After several times (usually 10−12 times) of penetration, when the tip of the glass probe was not broken any more, the outside diameter of the tip was recorded as the suitable tip size for that soil. In this study, a total 25 single- or double-barreled glass probes were tried for each soil, and the average size of the broken glass probes was considered as the suitable tip size for that soil.

**pH Microelectrodes.** Double-barreled pH ion-selective microelectrodes were used to measure the pH profiles. A double-barreled borosilicate glass tubing (2B150F-4, World Precision Instrument, Sarasota, FL) with an inside diameter (i.d.) of 0.8 mm and an outside diameter (o.d.) of 1.5 mm was first cleaned and treated by the chromic sulfuric solution (VWR, 9875) and alcohol (*41*). The glass tubing was pulled on a vertical micropipet puller with a "loop" filament (P-30, Sutter Instrument Co., Novota, CA), using the conditions of the highest heat (999), low onset of the hard pull (0.0), and high pull strength (650). The pulled micropipet tip (usually < 1 $\mu$m) was broken to a size of about 20−35 $\mu$m using a forceps and then further beveled to the required size (e.g., 35−40 $\mu$m). However, it is not necessary to bevel the glass pipet if an exact tip size is not required.

The next step was silanization. The trimmed (or beveled) glass pipets (usually about 6−8) were mounted vertically with their tips upward in an aluminum block ($w \times l \times h = 5 \times 5 \times 1$ cm$^3$) with both ends of the pipet open to the air. The block was placed on an aluminum pan in an oven at 168 °C. Subsequently, 0.5−1 mL of dimethyldichlorosilane (Sigma, No. 3879) was introduced below the block, and the aluminum pan was covered with a beaker that was silanized previously. The pipets were exposed to dimethyldichlorosilane vapor for 5−6 min. After that, the cover was removed, and the pipets were left in the oven for 2−3 h.

After silanization, one barrel, served as the working probe, was backfilled with a hydrogen ion-selective cocktail. The composition (w/w) of the pH cocktail was 2.85% hydrogen ion ionophore I (Fluka, No. 95292), 5% poly(vinyl chloride) (molecular weight PVC, Fluka, No. 81392), 0.5% potassium tetrakis(4-chlorophenyl)borate (Fluka, No. 60591), and 91.65% bis(1-butylpentyl) adipate (BBPA) (Fluka, No. 02150). The mixture was diluted 2−3 times its weight with tetrahydrofuran (Fluka, No. 87369) to stabilize the PVC. The barrel filled with the pH cocktail was then backfilled with a buffer solution (pH = 7), consisting of 0.04 *M* $KH_2PO_4$, 0.023 *M* NaOH, and 0.015 *M* NaCl (*17*). Another barrel, used as the reference probe, was filled with 3 *M* KCl saturated with AgCl and mixed with agar (0.5−1% w/w) (*17*). A piece of Ag/AgCl wire was inserted into each barrel to transport the millivolt signal generated between the working electrode and reference electrode to a Chemical Microsensor (see below).

The pH microelectrodes were calibrated using a series of pH buffer solutions (pH = 4, 7, and 10). The pH microelectrodes with their slopes greater than 58 mV/pH unit (the theoretical value is 59) were used for the pH measurement in soil samples. It should be pointed out that the slopes of these pH microelectrodes were slightly lower than 58 mV/pH unit if soil samples with moisture of 10−30% (w/w), instead of solution, were used as test materials. This might be due to the nonideal conditions, the interference of other ions, or the temperature. Therefore, to offset the effect of soil structure on the microelectrode readings, the pH microelectrodes, with their slopes greater than 58 mV/pH unit in the series of pH buffer solutions, were calibrated using a soil standard series. The soil standard series consisted of similar soils soaked in pH buffer solutions (pH = 4, 7, or 10) within three small containers (10 mL plastic beakers) (usually the final soil water content was of 20% w/w). The pH values of these soil standard were measured using a macro-pH probe (BK140608, VWR) with a pH meter (Beckman Φ100 ISFET pH Meter, Beckman Instruments, Inc., Fullerton, CA) specifically designed for soil application. The pH values measured were used as the standard pH to make the calibration curve from which the pH value of the tested soil sample can be determined.

**Redox Potential Microelectrodes.** Redox potentials were measured using the redox microelectrode with a tip size of 20−30 $\mu$m (o.d.), which was bound together with a custom-made reference electrode (Ag/AgCl, tip size 20 $\mu$m). The distance between the working redox microelectrode and the bound reference microelectrode was about 1.5 mm. All the redox data reported in this paper are relative to the Ag/AgCl reference microelectrode. Therefore, ORP rather than Eh, which indicates a potential with respect to a standard hydrogen electrode, is used in this paper to represent the measured potential value (*E*). Fabrication, calibration, and performance of the redox potential microelectrodes are presented elsewhere (*42*). The ORP microelectrodes were calibrated against redox potential standard solutions (*42, 43*). Readings for the same standard solution can vary with each fabricated microelectrode. Therefore, to compare redox

measurements in soil cores where more than one redox probe was used, all redox readings were converted to readings based on one electrode (*38*, *42*).

**ORP-pH Curve.** An artificial soil, consisting of 10 g of sand, 5 g of clay, and 7 mL of pH adjusting solution, was used to characterize the effect of pH on redox measurement in soils. Assuming that the solution can only change the pH value and has no effect on the redox potential of the soil, soil pH was adjusted using 0.01 *M*, 0.005 *M*, 0.00025 *M* HCl, deionized water, or 0.005 *M* and 0.01 *M* NaOH, respectively. The pH values of the artificial soils were measured using a macro-pH probe (Beckman Instruments, Inc., Fullerton, CA), and redox potentials were measured using the redox potential microelectrode described above. The pH values and corresponding redox potentials were used to construct ORP-pH curves for the artificial soil. These ORP-pH curves were then used to explore the effect of pH on redox measurements.

To construct an ORP-pH curve of the munitions-contaminated soil, approximately 7 $cm^3$ of previously vegetated soil was put into a small container (10 mL plastic beaker). The pH of the soil in the container was first adjusted to 9 or 10 with 0.1 N NaOH, and the corresponding redox potential was measured. The pH was then lowered by gradually adding 0.1 *M* HCl, and the corresponding redox potential was measured. The relationship between ORP and pH was determined using regression analysis.

**Microelectrode Measurement System.** The microelectrode system was grounded by a line inserted 2.4 m into the ground. The tray holding the soil sample was placed on a vibration-isolation table (Technical Manufacturing Corporation, Peabody, MA) inside a Faraday cage. The soil core was put horizontally within the tray; that is, the x−y plan shown in Figure 1 was perpendicular to the plan of the vibration-isolation table. The microelectrodes (pH or redox electrodes) were positioned manually using a 3-D micromanipulator (World Precision Instrument, Sarasota, FL). The signal generated from the microelectrodes was measured using a chemical microsensor (Diamond General, Ann Arbor, MI). The signal could then be recorded and analyzed using a data acquisition/control system that interfaced to a PC-computer with LabTech Notebook (*43*).

In this study, the electrode was thought stable if the differences between the readings obtained within 1 min were not greater than 3% (the corresponding rate of the electrode potential change was in a range of 0.5−3 mV/min). Usually, it took less than 2 min for the pH or ORP microelectrodes to become stable. The reading of one point in the soil sample was recorded 3−5 min after the microelectrode was inserted into the point. Usually, there was no drafting after the readings of the pH and ORP microelectrodes became stable. This might be due to the Faraday cage, good grounding, and stable microelectrodes. Reported pH or redox potential readings are the averages of a minimum of six readings within 3 min once the pH and redox potential microelectrode became stable. Differences between individual pH and redox potential readings were very small (standard deviations < 3%) (*42*, *43*).

## Results

**Radial and Longitudinal pH Distributions.** The soil pH varied little in the radial (horizontal or *x*/*y* directions shown in Figure 1) direction. For the vegetated soil, average pH for the most outer core (10 cm) at the different depths ranged from 5.09 and 6.01, with an overall average of 5.46. In the second core (7.5 cm), the average pH was 5.48 with a range of 5.00−6.40. In the third core (5 cm), the pH at different depths ranged from 6.38 to 4.80 with an average of 5.21, which was the lowest average among the four cores. For the fourth, innermost core, the pH ranged from 4.97 to 6.02 and the average was 5.39, higher than the average in the third core and slightly lower than averages in the first and second cores.

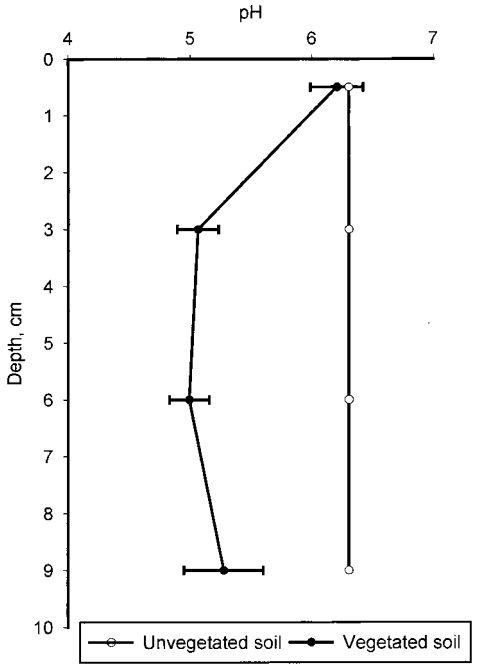


**FIGURE 2. The longitudinal distributions of pH in the vegetated soil compared with the pH values in the unvegetated soil. Data presented are average values of 16 readings at 4 different cores. Bars on symbols indicate standard deviations.**

Along the vertical (longitudinal or *z* direction shown in Figure 1) height of the vegetated soil sample, the highest average pH (6.20) appeared at the 0.5 cm depth. The lowest average pH (4.99) occurred between 3 and 6 cm below the soil surface (Figure 2); this region had the highest root density. This contrasts with the relatively uniform pH in the unvegetated soil (6.27−6.33), which was higher than the pH measured at any point in the vegetated soil (Figure 2).

**Influence of pH on Redox Potential.** Considering that both redox potential and pH vary in the rhizosphere, the effect of ambient pH on the effective redox potential can be determined by converting the measured redox potential values to a uniform pH, generally, pH 7. Based on eqs A2 or A6 shown in Appendix A, the following can be obtained

$$ORP_7 = ORP_0 + slope^*(pH_0 - 7) \qquad (1)$$

where $ORP_7$ is the ORP adjusted to pH = 7; $ORP_0$ is the original measured ORP; $pH_0$ is the pH value measured at the same point for $ORP_0$ measurement; and the slope is $[(2.303mRT)/(nF)]$ for direct participation of protons in the redox reactions, and $[(2.303nRT)/(nF)]$ for effects on the dissociation of the reductant. Theoretically, the slope is equal to 59.16 mV at 25 °C if both n and m equal 2 (*41*).

Note that the slope in eq 1 is a correction factor, ranging from −40 to −230 mV per pH unit (*41*). These can be seen from eqs A2 and A6, where *m* and *n* determine the slope in eq 1. Different soils may involve different redox reactions, and the m or *n* values may be different. Therefore, the relationship between ORP and pH must be characterized in each soil to obtain the appropriate slope. In this study, the ORP-pH curve had a slope of −55.50 mV/pH unit for the artificial soil and −115.24 mV/pH unit for the munitions-contaminated soil (Figure 3). This slope was used in eq 1 to convert the measured redox potentials to values based on the pH of 7. These results demonstrate that pH affects redox potential and that different soils may produce different slopes.

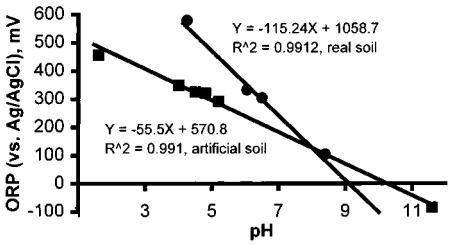


**FIGURE 3. ORP-pH curves for the artificial and field-collected soils.**

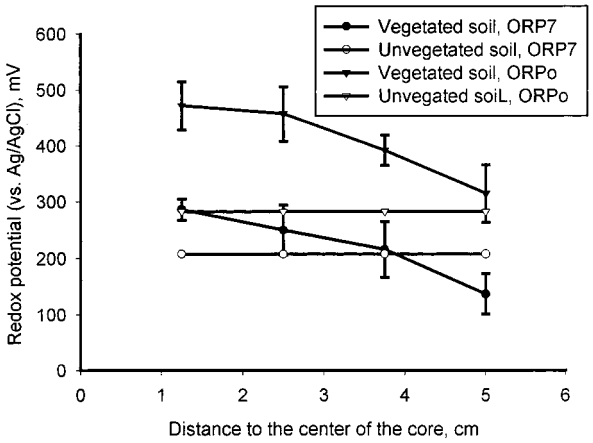


**FIGURE 4. The radial distributions of redox potential ($ORP_7$, adjusted to pH 7 and $ORP_0$, original measurement) in the vegetated soil compared with the unvegetated soil. Data presented are average values of 16 readings at four different depths of the same core. Bars on symbols indicate standard deviations.**

**Redox Potentials.** Since the pH was lower in the vegetated soil than in the unvegetated soil (Figure 2), the observed redox potential differences may be due in part to differences in pH. Equation 1 and the regression slope (−115.24 mV/pH unit) in Figure 3 were used to convert all measured redox potentials to values at pH = 7 ($ORP_7$)

In the radial (horizontal) direction, redox potentials increased in proximity to the plant (Figure 4). Note that the redox potentials in four cores of the vegetated soil are higher than in the unvegetated soil if the measured ORPs are not adjusted to pH 7. After adjustment, however, the redox potential in the first (10 cm) core of the vegetated soil was lower than in the unvegetated soil.

In the longitudinal direction, unadjusted redox potential increased with depth, while the $ORP_7$ readings showed a moderate reduction near the 3 cm depth (Figure 5). The top layer had the highest redox potentials, which may be due to oxygen diffusion from the atmosphere. The lowered redox potential near the 3 cm depth was likely due to microbial activity in the rhizosphere. In the unvegetated soil, a general decreasing redox potential with increasing depth was observed, which can be attributed to reduced transport of oxygen from the air to soil. However, there was almost no redox potential difference among different locations with the same depths.

## Discussion

**Important Factors Affecting Performance of pH and ORP Microelectrodes.** Three important factors were investigated: (1) suitable microelectrode tip sizes; (2) comparison of the new pH cocktail with the cocktail suggested by Fluka; and (3) the distance between the two electrodes.

The suitable tip size depended on soil and soil water content. For different soils or the same soils with different moisture, the suitable tip sizes were different (Figure 6(a)). The weight ratio of sand to clay can affect the suitable tip

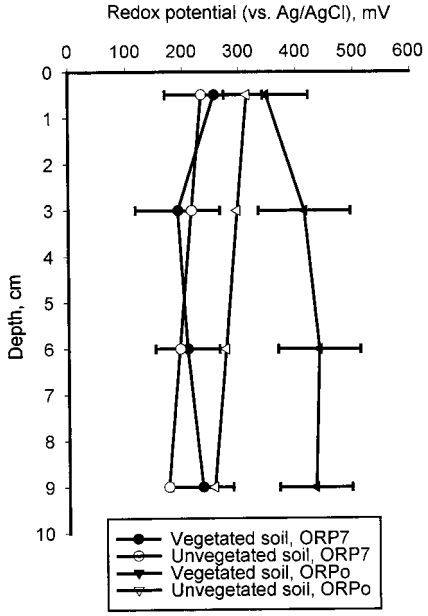


**FIGURE 5. The longitudinal distributions of redox potentials ($ORP_7$, adjusted to pH 7 and $ORP_0$, original measurement) in the vegetated soil compared to the unvegetated soil. Data presented are average values of 16 readings at the same depth of four different cores. Bars on symbols indicate standard deviations.**

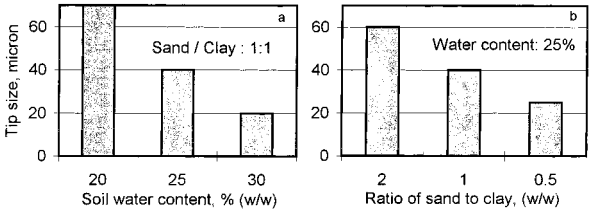


**FIGURE 6. Suitable tip size for different artificial soils with (a) different moisture contents (w/w) and (b) different sand-to-clay ratios (w/w).**

size of the microelectrode; the higher the ratio, the bigger the suitable tip size (Figure 6(b)). Therefore, it is necessary to determine the suitable tip size for different soil samples of interest. For the munitions-contaminated soil (with moisture content of 10% w/w), the suitable tip size was 35−40 $\mu$m for the pH microelectrode and 20−40 $\mu$m for the redox potential microelectrode (these microelectrodes have a metal alloy inside the glass probes, and therefore are sturdier).

The new pH cocktail developed in this study is different from that suggested by Fluka. The pH cocktail reported by Fluka (*44*) consisted of 1% hydrogen ion ionophore I, in 33% PVC, 65.5% BBPA, and 0.5% potassium tetrakis(4-chlorophenyl)borate. When used for soil samples, however, the slope produced by the pH microelectrode filled with the Fluka cocktail was approximately −30 to −40 mV/pH (−33.8mV/pH in Figure 7). According to the theory of the ion-selective microelectrode (*45*), the ideal slope, considering the effect of the interference ion, should be above −50 mV/pH when the temperature is 20 °C. The lower slope represents poor selectivity. The tip size (o.d.) is one of the principal factors affecting microelectrode performance (*17, 46*). In previous biofilm studies, the tip size (o.d.) was usually 1−5 $\mu$m (*14, 23−34*), which is much smaller than the size used in this study. In addition, the Fluka cocktail is very sticky, making it difficult to backfill into the probe. In this study, the optimum cocktail composition was determined by changing the relative concentration of the four chemicals. The slopes for all of the pH microelectrodes were ≥ −52 mV/pH units (see the example in Figure 7); the average slope of these pH

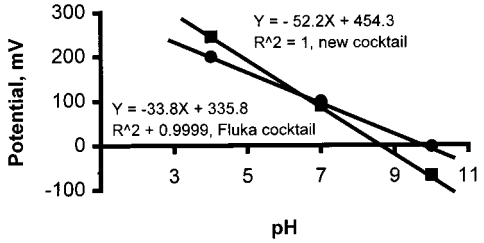


**FIGURE 7. Comparison between the Fluka's cocktail and the cocktail developed in this study.**

**TABLE 1. Effect of the Distance between the Working and Reference Microelectrodes on Potential Readings**

| | | | | | |
|---|---|---|---|---|---|
| distance cm | | 0.5 | 1.5 | 2.5 | 1.5 |
| microelectrode | ORP | 285 | 302 | 308 | 277 |
| readings, mV | PH | 88 | 93 | 102 | 75 |

microelectrodes was −55.8 mV/pH units with a standard deviation of 3 mV/pH units (data not shown). The performance of the pH microelectrode filled with this new cocktail was stable and satisfactory for soil samples.

The effect of the distance between the two electrodes on signal readings was also evaluated. Initially, a separated macro reference electrode (Ag/AgCl, MI-401 Micro-Reference Electrode (no. 47926), Microelectrodes, Inc., Bedford, NH) was coupled to a working microelectrode. For the soil samples, which usually have low conductivity, the distance between the working electrode and reference electrode can greatly affect the final readings. Different readings were obtained for the same point when the position of the reference electrode was changed (Table 1). Therefore, the distance between these two electrodes must be fixed and minimized. For this reason, double-barreled glass tubing was used to construct the pH microelectrode. For the redox microelectrode, the reference microelectrode was taped to the working microprobe due to the difficulty in constructing a double-barreled redox microelectrode (*43*). In this study, the distance between the working probe and reference probe was $< 5\,\mu$m for the pH microelectrode and about 1.5 mm for the redox potential microelectrode.

**pH and ORP Distributions.** Information obtained in this study on pH distributions in vegetated soils is consistent with previous studies (*1, 37*−*39*). Marschner (*1*) reported that the rhizosphere pH may differ from the bulk soil pH by up to two units, depending on plant and soil factors. Yang et al. (*38*) reported the microscale spatial variability of soil pH. A comparison between pH values in vegetated and unvegetated soil indicates that the plant and its associated microbial community are the major reasons for pH decreases in the rhizosphere. Differences in the pH may also reflect the impacts of plants, soil fauna, and/or precipitation on the soil. The most important factors for root-induced changes in rhizosphere pH are imbalances in cation/anion uptake and corresponding differences in the net release of $H^+$ and $HCO_3^-$ (or $OH^-$), and the release of organic acids resulted from microbial activity (*1*). The initial pH and buffering capacity of the soil are also important factors affecting changes in rhizosphere pH.

Two perspectives may be taken on measurement and interpretation of redox potentials in a vegetated-soil system. The system may be simply treated as a black box by measuring redox without linking to pH, this "effective" value reflects in situ redox potential in the system. A preferred approach treats the vegetated-soil system as a gray box in which redox potential is related to pH, as shown in eq 1. The different profiles shown by the original and converted readings of redox potentials (Figures 4 and 5) demonstrate the importance of obtaining information on both pH and redox potentials.

It should be noted that the redox potential is oxygen-dependent due to the fact that the ORP-pH boundary for the upper stability field of water is governed by (*47*)

$$4H^+ + O_2(g) + 4e^- = 2H_2O \qquad (2)$$

In this study, the redox measurements were conducted by cutting the soil core from 10 × 10 × 10 (cm) to 7.5 × 7.5 × 10 to 5 × 5 × 10 to 2.5 × 2.5 × 10. For each cutting, the redox and pH values at 16 sampling points were measured under the same atmospheric conditions (e.g., $Po_2$ is about 0.2 bar). Therefore, oxygen did not affect the relative values of the redox data obtained in this study, and the effect of oxygen concentrations on the measurement of redox potentials is not discussed in this paper.

**TNT and RDX Concentrations in Vegetated and Unvegetated Soil.** Based on measurements, TNT and RDX concentrations (all in mg/kg) were only 63.0 and 1234 for vegetated soil no. 1 (Lambs Quarters plants), 20.0 and 285 for vegetated soil no. 2 (Daily Fleabane plants), and 25.0 and 297 for vegetated soil no. 3 (Ragweed plants). However, TNT and RDX concentrations (all in mg/kg) in unvegetated soil were 4564 and 4488, respectively. Considering that the distance between the vegetated soil and the unvegetated soil was about 1 foot, it can be surmised that the rhizosphere has some impact on contaminant degradation. In the future, the effects of ORP or pH on bioremediation should be evaluated so that information on the variability in pH and ORPs in rhizosphere soil might be used to explain, in part, greater degradation of xenobiotics in the presence of plant roots than in their absence.

## Summary

Conventional bulk soil batch measurements may not reveal the true variability in pH and redox potential in the rhizosphere. Microelectrodes are powerful analytical tools that can be used to accurately measure microscale pH and redox potential in these environments. Application of this technique revealed that vegetated soil contaminated with TNT and RDX had lower pH values than unvegetated soil. While no radial difference in pH was apparent in the vegetated soil, the pH was highest at the soil surface and lowest near the root tips. In unvegetated soil, no radial or longitudinal pH differences were observed.

The redox potential of a given redox system is pH-dependent. To interpret soil redox potential, it is recommended that pH be measured along with redox potential at the same positions. The profiles based on original redox readings are different from those based on redox potentials adjusted to pH 7.

In the vegetated soil, redox potentials (normalized for equivalent pH) increased in proximity to the plant. Redox potential was the highest at the 0.5 cm depth and lowest at the 3 cm depth. Except for layer 2 (3 cm depth) and core 1 (10 cm), the redox potential of all other layers and cores in the vegetated soil were higher than in the unvegatated soil. The redox potential in the unvegetated soil decreased with depth.

## Acknowledgments

This work was funded by NSF/EPSCoR cooperative agreement EPS-9255225, the College of Engineering and Technology, the Center for Infrastructure Research, the Water Center, and the Civil Engineering Department of the University of Nebraska-Lincoln(UNL). The authors would like to express their deepest appreciation to Drs. S. Comfort and P. Shea and Mr. J. Shan of the UNL for their help in providing the

analysis of TNT and RDX and the great assistance in writing and editing this paper.

## Appendix A

This appendix describes further details of influence of pH on redox potential.

In addition to electron transfer, protons may directly or indirectly affect oxidation−reduction reactions. For direct participation of protons in a redox reaction (*41*)

$$\text{reductant} + x\text{H}_2\text{O} \leftrightarrow \text{oxidant} + m\text{H}^+ + n\text{e}^- \quad \text{(A1)}$$

and

$$\text{Eh} = E^0 + \frac{2.303RT}{nF}\left\{\log\left(\frac{[\text{oxidant}]}{[\text{reductant}]}\right) - m\text{pH}\right\} \quad \text{(A2)}$$

where Eh is the redox potential (mV); $E^0$ is the standard redox potential (mV); $n$ is the number of electrons involved in the reaction; $m$ is the number of protons involved in the reaction; x is the stoichiometric coefficient for $H_2O$; $F$ is Faraday's constant (96 500 coulombs/equivalent); [oxidant] and [reductant] are the representative molar concentrations of oxidant and reductant.

For the dissociation of the reductant

$$\text{H}_n\text{-reductant} \leftrightarrow \text{reductant}^{n-} + n\text{H}^+ \quad \text{(A3)}$$

At equilibrium

$$K = \frac{[\text{reductant}^{n-}][\text{H}^+]^n}{[\text{H}_n\text{-reductant}]} \quad \text{(A4)}$$

where [reductant$^{n-}$], [$H^+$], [$H_n$-reductant] are molar concentrations. Assuming that the oxidant is reduced to reductant$^{n-}$ after gaining $n$ electrons, and if the total concentration of the reductant, $[\text{reductant}]_T$ is the sum of [reductant$^{n-}$] and [$H_n$-reductant], based on eq A4, we have

$$[\text{reductant}^{n-}] = \frac{K[\text{reductant}]_T}{\text{K} + [\text{H}^+]^n} \quad \text{(A4′)}$$

Based on the definition of Eh and eq A4′, the Eh would be

$$\text{Eh} = E^0 + \frac{2.303RT}{nF}\left\{\log\left(\frac{[\text{oxidant}]}{[\text{reductant}]_T}\right) + \log(K + [\text{H}^+]^n) - \log K\right\} \quad \text{(A5)}$$

This equation shows that the relative magnitude of $K$ and [$H^+$] determines the effect of protons on ORP. When $K \ll [\text{H}^+]^n$, the $K$ in $\log(K + [\text{H}^+]^n)$ can be neglected and the term of $[(2.303RT)/(nF)]\log K$ can be combined into $E^{0\prime}$. Therefore, eq A5 becomes

$$\text{Eh} = E^{0\prime} + \frac{2.303RT}{nF}\left\{\log\left(\frac{[\text{oxidant}]}{[\text{reductant}]_T}\right) - n\text{pH}\right\} \quad \text{(A6)}$$

Equations A2 and A6 demonstrate that, at a fixed ratio of the oxidized form to the reduced form, the higher the concentration of protons, the more positive the electrode potential.

When pH equals $pH_0$ and 7, eq A2 will be

$$\text{Eh}_0 = E^0 + \frac{2.303RT}{nF}\left\{\log\left(\frac{[\text{oxidant}]}{[\text{reductant}]}\right) - m\text{pH}_0\right\} \quad \text{(A2′)}$$

$$\text{Eh}_7 = E^0 + \frac{2.303RT}{nF}\left\{\log\left(\frac{[\text{oxidant}]}{[\text{reductant}]}\right) - m7\right\} \quad \text{(A2″)}$$

Equation A2″ − equation A2′ gives

$$\text{Eh}_7 = \text{Eh}_0 + m^*\{[2.303RT]/[nF]\}^*(\text{pH}_0 - 7) \quad \text{(A8)}$$

Similarly, based on eq A6, we have

$$\text{Eh}_7 = \text{Eh}_0 + n^*\{[2.303RT]/[nF]\}^*(\text{pH}_0 - 7) \quad \text{(A8′)}$$

Therefore, for both cases, we have

$$\text{Eh}_7 = \text{Eh}_0 + \text{slope}^*(\text{pH}_0 - 7) \quad \text{(A8″)}$$

which is eq 1 in the text.

## Literature Cited


(1) Marschner H. *Mineral Nutrition of Higher Plants*; Academic Press: 1995; pp 509−595.
(2) Brown, K. T.; Flaming, D. G. *Advanced Micropipet Techniques for Cell physiology*; John Wiley & Sons: 1986.
(3) Thomas, R. C. *Ion-selective intracellular Microelectrodes: how to make and use them*; Academic Press: New York, 1978.
(4) De Beer, D: van den Heuvel, J. C. *Anal. Chem. Acta* **1988**, *213*, 259−265.
(5) De Beer, D. Ph. D. dissertation, University of Amsterdam, The Netherlands, 1990.
(6) De Beer, D.; Huisman, J. W.; van den Heuvel, J. C., and Ottengraf, S. P. P. *Water Res.* **1992**, *26*, 1329−1336.
(7) Zhang, T. C.; Bishop, P. L. *Water Environ. Res.* **1996**, *68*(7), 1107−1115.
(8) Lewandowski, Z.; Walser, G.; Characklis, W. G. *Biotech. Bioeng.* **1991**, *38*, 877−882.
(9) Lweandowski, Z.; Walser, G.; Larsen, R.; Peyton, B.; Xharacklis, W. G. *Proceedings of the 90th ASCE National Conference on Environmental Engineering*; 1990; pp 17−24.
(10) Revsbech, N. P.; Jorgensen, B. B.; Blackburn, T. H. *Limnol. Oceanogr.* **1983**, *28*, 1062−1074.
(11) Revsbech, N. P.; Nielsen, L. P.; Christensen, P. B.; Sorensen, J. *Appl. Environ. Microbiol.* **1988**, *47*, 2245−2249.
(12) Revsbech, N. P. In *Structure and Function of Biofilms*; Characklis, W. G., Wilderer, P. A., Eds.; John Wiley & Sons Ltd.: pp 129−144.
(13) Fu, Y. Z.; Zhang, T. C.; Bishop, P. L. *First International Specialized Conference on Biofilm Reactors*; Paris, France, 1993; pp 543−550.
(14) Zhang, T. C.; Bishop, P. L. *Water Environ. Res.* **1995**, *67*, 992−1003.
(15) Zhang, T. C.; Bishop, P. L. *Water Sci. Technol.* **1993**, *29*, 335−344.
(16) Fu, Y. Z. Ph.D. Dissertation, University of Cincinnati, OH, 1993.
(17) Zhang, T. C. Ph.D. Dissertation, University of Cincinnati, OH, 1994.
(18) Hooijmans, C. M.; Geraats, S. G. M.; Potters, J. J. M.; Luyben, K. *Chem. Eng. J.* **1990**, *44*, B41-B46.
(19) Hooijmans, C. M.; Geraats, S. G. M.; Luyben, K. *Biotech. Bioeng.* **1990**, *35*, 1078−1087.
(20) Henriksen, C. M.; Bloom, A. J.; Spanswick, R. M. *Plant Physiol.* **1990,** *93*, 271−280.
(21) Latifi, M. A.; Midoux, N.; Storck, A. *Chem. Eng. Sci.* **1989**, *44*(11), 2501−2508.
(22) Latifi, M. A.; Rode, S.; Midoux, N.; Storck, A. *Chem. Eng. Sci.* **1989**, *47*(8), 1985−1992.
(23) Costerton, J. W.; Lewandowaski, Z.; Caldwell, D. E.; Korber, D. R.; Lappio-Scott, H. M. *Annu. Rev. Microbiol.* **1995**, *49*, 711−745.
(24) De Beer, D.; Stoodley, P.; Roe, F. L.,; Lewandowski, Z. *Biotech. Bioeng.* **1994**, *43*, 1131−1138.
(25) Yang, S.; Lewandowski, Z. *Biotech. Bioeng.* **1995**, *48*, 737−744.
(26) Abrahamson, M.; Lewandowski, Z.; Geesey, G.; Shjak-Brak, G.; Strand, W.; Christensen, B. E. *J. Microbiol. Methods* **1996**, *26*, 161−169.

(27) De Beer, D.; Stoodley, P.; Lewandowski, Z. *Biotech. Bioeng.* **1996**, *53*, 151−158.
(28) Stewart, P. S.; Hamilton, M. A.; Goldstein, B. R. *Biotech. Bioeng.* **1996**, *49*, 445−455.
(29) Chen, X.; Stewart, P. S. *Environ. Sci. Technol.* **1996**, *30*(6), 2078−2083.
(30) Xu, X.; Stewart, P. S.; Chen, X. *Biotech. Bioeng.* **1996**, *49*, 93−100.
(31) Lewandowski, Z.; Dickinson, W.; Lee, W. *Water Sci. Technol.* **1997**, *36*(1), 295−302.
(32) Yu, T.; Bishop, P. L. *Water Sci. Technol.* **1998**, *37*(4−5), 195−198.
(33) Bishop, P. L.; Yu, T. *IAWQ Specialty Conference on Microbial Ecology of Biofilm: Concepts, Tools and Applications*; Lake Bluff, IL, Oct. 8−10, 1998.
(34) Yu, T.; Bishop, P. L. *Proceedings of WEFTEC'97*, Vol. 1, 70th Annual WEF Conference, Chicago, IL, Oct. 18−22, **1997**; pp 73−82.
(35) Sexstone, A. J.; Revsbech, N. P.; Parkin, T. B.; Tiedje, J. M. *Soil Sci. Soc. Am. J.* **1985**, *49*, 645−651.
(36) Flessa, H.; Fischer, W. R. *Plant Soil* **1992**, *143*, 58−62.
(37) Conkling, B. L.; Blanchar, R. W. *Soil Sci. Soc. Am. J.* **1989**, *53*, 58−62.
(38) Yang, J.; Hammer, R. D.; Blanchar, R. W. *Soil Science* **1995**, *160*, 371−375.
(39) Yang, J.; Blanchar, R. W.; Hammer, R. D. *Soil Sci. Soc. Am. J.* **1994**, *58*, 354−357.
(40) Hundal, L. S.; Singh, J.; Bier, E. L.; Shea, P. J.; Comfort, S. D.; Powers, W. L. *Environmental Pollution* **1997**, *97*, 55−64.
(41) Yu, T. R.; Ji, G. L. *Electrochemical methods in soil and water measurement*; Pergamon Press: 1997; pp 297−313.
(42) Pang, H.; Zhang, T. C. *Environ. Sci. Technol.* **1998**, *32*, 3646−3652.
(43) Pang, H. M.S. Thesis, University of Nebraska-Lincoln, 1997.
(44) Fluka *Inonophores* **1988**, 15−16.
(45) Admstrong, W. M.; Garcia-Diaz, J. F. *Federation Proc.* **1980**, *39*, 2851−2859.
(46) Henriksen, G. H.; Bloom, A. J.; Spanswick, R. M. *Plant Physiology*. **1990**, *93*, 271−280.
(47) Langmuir, D. *Aqueous Environmental Geochemistry*; Prentice Hall: 1997.

*Received for review October 15, 1998. Revised manuscript received January 22, 1999. Accepted January 26, 1999.*

ES981070X